Adsorption (2013) 19:465–474
DOI 10.1007/s10450-012-9468-1

Magnetite nanoparticles for removal of heavy metals from aqueous solutions: synthesis and characterization

Liliana Giraldo · Alessandro Erto · Juan Carlos Moreno-Piraján

Received: 29 September 2012 / Accepted: 29 December 2012 / Published online: 12 January 2013

Abstract Fe_3O_4 magnetic nanoparticles were synthesized by co-precipitation method. The structural characterization showed an average nanoparticle size of 8 nm. The synthesized Fe_3O_4 nanoparticles were tested for the treatment of synthetic aqueous solutions contaminated by metal ions, i.e. Pb(II), Cu(II), Zn(II) and Mn(II). Experimental results show that the adsorption capacity of Fe_3O_4 nanoparticles is maximum for Pb(II) and minimum for Mn(II), likely due to a different electrostatic attraction between heavy metal cations and negatively charged adsorption sites, mainly related to the hydrated ionic radii of the investigated heavy metals. Various factors influencing the adsorption of metal ions, e.g., pH, temperature, and contacting time were investigated to optimize the operating condition for the use of Fe_3O_4 nanoparticles as adsorbent. The experimental results indicated that the adsorption is strongly influenced by pH and temperature, the effect depending on the different metal ion considered.

Keywords Magnetite · Nanoparticles · Isotherms · Metal ions

L. Giraldo
Departamento de Química, Universidad Nacional de Colombia, Bogotá, Colombia

A. Erto
Dipartimento di Ingegneria Chimica, Università degli Studi di Napoli Federico II, Naples, Italy

J. C. Moreno-Piraján (✉)
Departamento de Química, Universidad de los Andes, Bogotá, Colombia
e-mail: jumoreno@uniandes.edu.co

1 Introduction

Adsorption processes are worldwide adopted in the field of environmental protection, thanks to the ability of certain solids to preferentially concentrate onto their surface specific substances, such as heavy metals and organics. A wide range of adsorbents have been developed and tested, including several activated carbons for the removal of pollutants from wastewaters (Faur-Brasquet et al. 2002; Mohan and Singh, 2002; Puziy et al. 2004; Di Natale et al., 2009; Moreno-Piraján and Giraldo 2012). During the last 10 years, extensive researches have been carried out to find low-cost and high capacity adsorbents for water remediation. A large number of low-cost agricultural wastes, mud (Keith and McKay 2008; Purevsuren et al. 2004), tire rubber and fly ash (Jiang 2001; Wilson et al. 2003; Wu et al. 2005; Nasiruddin Khan and Farooq Wahab 2007; Balsamo et al. 2011) have been used for the removal of metal ions from polluted water. Several natural resources have been also studied including tree fern (Pattanayak et al. 2000; Moreno et al. 2010), peat, chitosan, coal and bone char (Pattanayak et al. 2000) or minerals such as sodium and calcium bentonite (Liu et al. 2007).

The efforts to find alternative low-cost materials and the recent progress of nano-techniques have led to the development of new classes of nanoparticles for the treatment of contaminated water. Nanoparticles, often characterized by large specific surface area, have attracted great interest because of their unique properties and potential applications.

Metal oxide nano-adsorbents have been extensively studied as they show very attractive properties compared to their bulk form, such as high adsorption capacity, enhanced catalytic activity, high dispersion degree and superparamagnetism behavior (Banfield and Zhang 2001;

Niemeyer 2001; Roco 2003; Savage and Diallo 2005; Waychunas et al. 2005; Perez, 2007; Nassar et al. 2011a, b). These properties offer novel applications for nano-adsorbents in many fields such as electronics, biotechnology, medicine, heavy oil upgrading, air pollution control and, in particular, for water treatment (Goya et al. 2003; Hua et al. 2009; Kang et al. 2005; Pankhurst et al. 2003; Portet et al. 2001; Reimer and Weissleder 1996; Häfeli et al. 1997). For an instance, magnetic iron oxide (Fe_3O_4) nanoparticles have been investigated not only in the field of magnetic recording but also in the areas of medical care and magnetic sensing in the recent decades (Shen et al. 2009; Sun et al. 2000; Xie et al. 2007; Pankhurst et al. 2003). It is believed that these magnetic nanoparticles exhibit amphoteric surface activity, easy dispersion ability and, thanks to their very small dimensions, a high surface-to-volume ratio, resulting in a high metal adsorption capacity (Shen et al. 2009; Nassar, 2011; Tratnyek and Johnson 2006; Sun and Zeng 2002; Si et al. 2004; Wan et al. 2006).

The use of magnetic nanoparticles for separation and preconcentration in analytical chemistry provides a new methodology that is faster, simpler and more precise than those used traditionally. The greatest advantage of this method is that desired materials are separated from solution by a simple and compact process while fewer secondary wastes are produced. Other advantages are represented by a large active surface area for given mass of particles and the ability to process solution that contains suspended solids (Khajeh and Khajeh 2009). In addition, an easy separation of the metals loaded on the magnetic adsorbent from solution can be achieved using an external magnetic field. Thus, an efficient, economic, scalable and non-toxic synthesis of Fe_3O_4 nanoparticles is highly desired for practical applications and fundamental research. A possible application of this sorbent should start from a thorough analysis of the main parameters influencing the adsorption of heavy metals on magnetite nanoparticles. Moreover, the individuation of the main adsorption mechanisms should take into account a quite large number of metal ions, so to allow a comparative analysis too. At the moment, there is still a lack of this information in the pertinent literature.

In this work, the feasibility of Fe_3O_4 nano-adsorbents for the removal of different metal ions, i.e. lead, zinc, copper, and manganese from aqueous solutions has been investigated. An accurate preparation procedure and a thorough characterization of the Fe_3O_4 nanoparticles has been provided. Adsorption tests have been carried out by varying solution pH, contact time and temperature. A critical interpretation of the experimental results allowed the identification of the field of potential application of iron oxide nano-adsorbents for metal adsorption from industrial wastewater.

2 Experimental

2.1 Sample preparation

Fe_3O_4 magnetite nanoparticles were synthesized by co-precipitation method (Shen et al. 2009). The procedure followed for the preparation is here specified, indicating the actual quantity of reagents used in the present work. A volume of 100 mL of ferric chloride (0.5 M) was added to 200 mL of ferrous chloride solution (0.5 M) and 150 mL of ammonium hydroxide (1 M). 300 mL of deionized water was deoxygenated by bubbling N_2 gas for 30 min in a 1000 mL flask and then added to the solution. Subsequently, 50 mL of ammonium chloride was added and the mixture was stirred magnetically for 10 min under a nitrogen atmosphere. Afterwards, 50 mL of ferrous chloride 0.5 M and 50 mL of ferric chloride 0.5 M were added and then the resultants were aged for 10 min before being separated. Below it is reported the reaction for the formation of Fe_3O_4 particles (Palacin et al. 1996):

$$Fe^{2+} + 2Fe^{3+} + 8NH_3 \cdot H_2O = Fe_3O_4 \downarrow + 8NH_4^+ + 4H_2O \quad (1)$$

Finally, the Fe_3O_4 product was separated by a centrifugal pump and washed twice with deionized water and ethanol. The obtained fine Fe_3O_4 nanoparticles were dried at 60 °C for 8 h (Shen et al. 2009).

2.2 Sample characterization

Fourier transform infrared spectroscopy (FTIR) spectra was performed on previously dried magnetite sample using a FTIR spectrophotometer (Model NICOLET5700, USA) in wave range of 3,500–400 cm^{-1} with a resolution of 4 cm^{-1}. The dried sample was placed on a silicon substrate transparent to infrared, and the spectra were measured according to the transmittance method. In addition, a GL-16A high-speed centrifuge (Shanghai) was used for separating the solid from the liquid during the sample preparation. The micrographs of prepared nanoparticles were obtained using a JSM-7001F scanning electron microscopy (SEM) and a Tecnai G2 20 transmission electron microscopy (TEM) was used for the characterization of nanoparticle size. Specific (BET) and external nanoparticle surface areas were measured by nitrogen adsorption and desorption at 77 K, using a Autosorb 3B (Quantachrome, MI, FL, USA) analyzer. The samples were degassed at 423 K under N_2 flow overnight before analysis. Surface area was calculated using the BET equation. The total pore volume, V_{pore}, was evaluated from nitrogen uptake at a relative pressure of ca. 0.97, using the adsorption branch. N_2 adsorption measurements were performed in duplicate to check the proper functioning of the

equipment and the entire technique, and the average values have been presented. The crystallographic phase was also determined by analyzing the X-ray powder diffraction taken with a PW 1830 diffractometer (Rigaku PDLX, Japan), using a monochromatized X-ray beam with nickel-filtered CuKα radiation (λ = 0.154021 nm).

2.3 Adsorbates

The following chemicals were used as precursor salts for the metal cations used in the experimental tests, namely $Cu(NO_3)_2{\cdot}5H_2O$ (99.9985 %, Merck, Germany), $Pb(NO_3)_2$ (99,9 %, Fisher Scientific, Toronto, ON, Canada) $Zn(NO_3)_2{\cdot}5H_2O$ (99 %, Fisher Scientific) and $Mn(NO_3)_2{\cdot}4H_2O$ (Merck, Germany). Individual stock solutions were prepared by dissolving a specified amount of the corresponding metal salt in 250 mL of deionized water, subsequently diluted to the required concentration. All metal salts were used without further purification (Shen et al. 2009).

2.4 Adsorption procedure

Thermodynamic and kinetic adsorption tests were performed in batch-mode; for all the experimental runs the procedure described by Nassar (2011) was followed. In a typical experiment, 200 mg of Fe_3O_4 nanoadsorbent were weighed into a 100 mL vial containing 50 mL of metal ion solution. Metals concentration ranged from 10 to 600 mg L^{-1}, in order to investigate a broad spectrum of concentrations.

Tests aimed at the analysis of pH effect were conducted at 298 K and the initial pH of the solution was adjusted without a significantly change in the initial concentration of metal ions in solution. Standard 0.1 M HCl and 0.1 M NaOH solutions were used for pH adjustment.

The effect of temperature was investigated as well, and adsorption tests were carried out at 288, 293, 313 and 323 K.

When adsorption equilibrium was reached, the nanoadsorbent was conveniently separated via external magnetical field and the solution was filtered to allow metal concentration measurements.

For the adsorption kinetic studies, metal ion initial concentration was set to 150 mg L^{-1} for each metal, and the experiments were carried out in a temperature incubator at 298 K, 200 rpm and solution pH 5.5. In order to determine the time required to reach the adsorption equilibrium, samples were analyzed for metal ion concentration at predetermined time intervals. To assure the accuracy, reliability, and reproducibility of the collected data, all batch tests were performed in triplicate and average values only were reported. Blank tests were run in parallel on metal solutions without addition of sorbent, showing that the experimental procedure does not lead to any reduction of metal concentration and pH variation unrelated to sorbent effects.

For all the tests, the concentration of metal ions in the supernatant was measured by a plasma-atomic emission spectrometer (ICP-AMS, Optima 3000XL, PerkinElmer) in accordance with the Standard Methods for water (American Public Health Association 1995).

The adsorbed amount of metal ions (mg of metal ion g^{-1} of Fe_3O_4 nanoadsorbent) was determined by the mass balance reported in Equation (2):

$$Q_e = \frac{C_o - C_e}{m} V \tag{2}$$

where C_o is the initial metal ion concentration in the supernatant (mg L^{-1}), V is the sample volume (L), and m is the mass of Fe_3O_4 nanoadsorbent (g). For time-dependent data, C replaces C_e and Q replaces Q_e in Equation (2).

3 Results and discussion

3.1 Fe_3O_4 magnetite nanoparticles characterization

FTIR spectrum in Fig. 1 shows that the H–O–H bending vibration at about 1,000–1,600 cm^{-1}, typical of the H_2O molecule, has very low intensity. Additionally, the second absorption band, between 900 and 1,000 cm^{-1}, corresponds to bending vibration associated to the O–H bond. The O–H in plane and out of plane bonds appear at 1,583.45–1,481.23 and 935.41–838.98 cm^{-1}, respectively (Nassar et al. 2011b). For strong hydrogen bridges, its maximum lies at about 900–1000 cm^{-1}. These first two bands correspond to the hydroxyl groups attached to the hydrogen bonds in the iron oxide surface, as well as the water molecules chemically adsorbed to the magnetic particle surface. In the spectrum showed (Fig. 1), the sample exhibits two intense peaks, respectively at 582 and 640 cm^{-1} bands, that are due to the stretching vibration mode associated to the metal–oxygen absorption band (Fe–O bonds in the crystalline lattice of Fe_3O_4) (Ahn et al. 2003). They are characteristically pronounced for all spinel structures and for ferrites in particular. This occurs because of the contributions, in these regions, deriving from the stretching vibration bands related to the metal in the octahedral and tetrahedral sites of the oxide structure. Moreover, the FTIR spectrum shows an absorption band at 1,706 cm^{-1}, which corresponds to the stretching vibration of the carboxyl group (C=O), associated to the oleic acid molecule, adsorbed onto the surface of the crystallites. Summarizing, magnetite nanoparticles have crystalline structure of inverse spinel

type, and FTIR absorption spectroscopy allowed identifying characteristic features of the spinel structure, as well as a presence of certain types of chemical substances adsorbed on the surface of nanoparticles (Ahn et al. 2003; Farmer 1974, 1982).

The magnetite sample was characterized by X-ray powder diffraction (XRD) with the corresponding results displayed in Fig. 2. The diffraction pattern and the relative intensities of all the diffraction peaks are typical of the magnetite and match those synthesized in this research.

Furthermore, the sample shows some of the characteristics of the bulk magnetite crystallite phase, with the broad peaks suggesting the nano-crystallite nature of the magnetite particles (González et al. 2010).

The resulting mean particle diameter of magnetite nanoparticles, as calculated from the Scherrer equation, was ca. 10 nm. This was in agreement with the result obtained from the TEM image (Fig. 3). From this image and from the corresponding electron diffraction pattern, it was determined that the magnetite particles are spherical with an average diameter of 8 nm. The corresponding BET specific surface area of the particles was 95.5 m^2 g^{-1}, as determined by conventional method.

The SEM analysis shown in Fig. 4 almost confirmed the results of the TEM analysis, as particle sizes in the range 10–70 nm were measured.

3.2 Adsorption tests: effect of contact time

The adsorption efficiency (η) can be defined as:

$$\eta = \frac{C_i - C_f}{C_i} \times 100 \quad (3)$$

where C_i and C_f represent initial and final metal ion concentration, respectively.

In order to determine the effect of contact time on Pb(II), Mn(II), Cu(II) and Zn(II) ions adsorption efficiency and to determine the time required to reach equilibrium, experimental tests were carried out using 200 mg Fe_3O_4 nanoparticles and 1:4 liquid to solid ratio (L/S) at 298 K and pH 5.5, with a contact time varied in the range of 2–48 h.

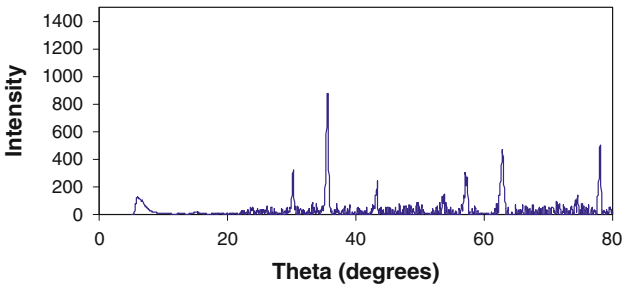

Fig. 2 XRD pattern for magnetite particles

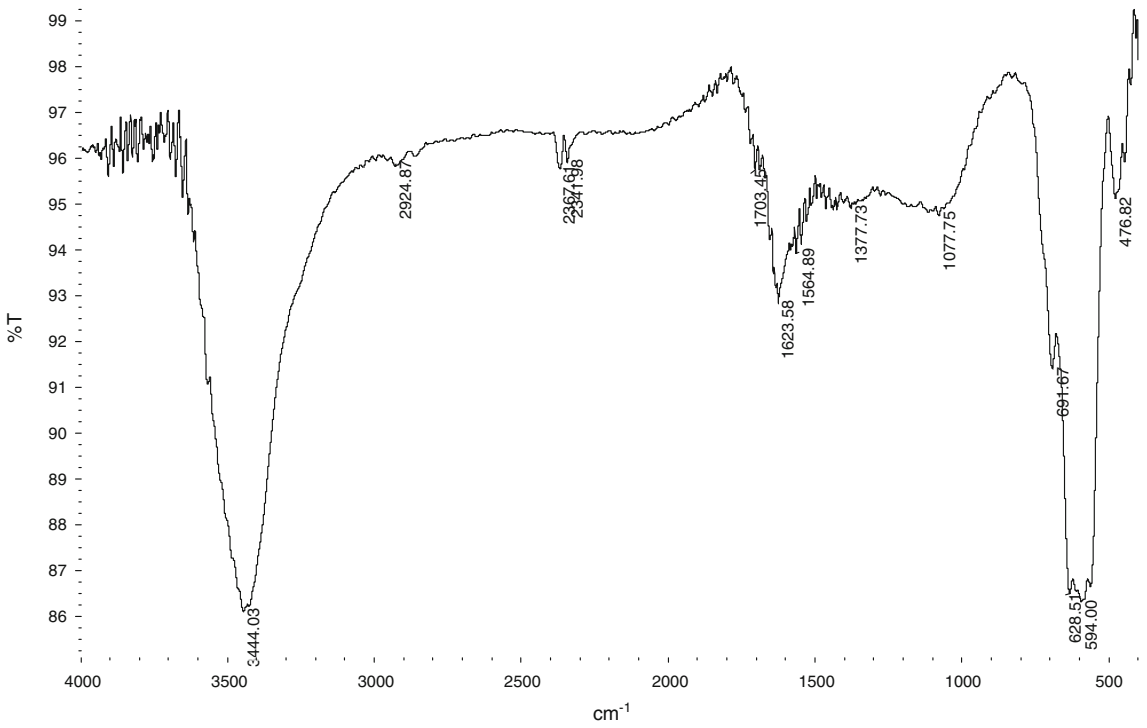

Fig. 1 FTIR spectra of magnetic Fe_3O_4 nanoparticles synthesized

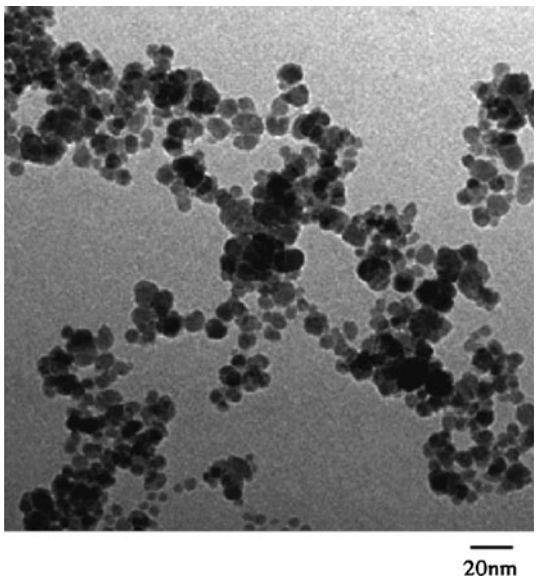

Fig. 3 Transmission electron microscope (TEM) imagen for magnetic Fe_3O_4 nanoparticles synthesized

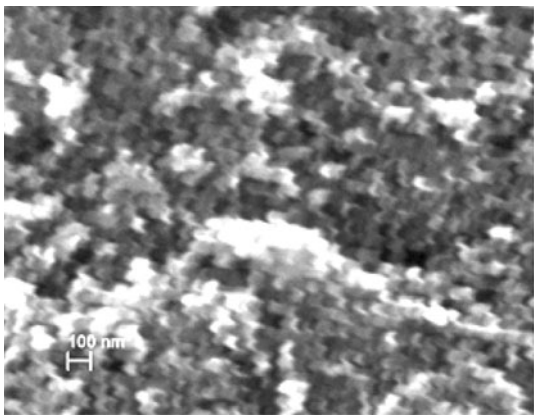

Fig. 4 SEM of image magnetic Fe_3O_4 nanoparticles synthesized

Figure 5 shows the effect of contact time on the adsorption efficiency of Pb(II), Cu(II), Zn(II) and Mn(II). It is clear that the adsorption efficiency of Zn(II) and Mn(II) were highly time dependent, i.e., a longer contact time resulted in higher adsorption efficiency. It can also be observed that a contact time of 24 h is sufficient to reach the equilibrium for all the investigated ions. Very interestingly, the adsorption efficiency of Pb(II) and Cu(II) were extremely high for very low time (<10 h) and remained constant in the whole range of the time investigated.

3.3 Adsorption kinetics

In order to better analyze the rates of Mn(II), Zn(II), Cu(II) and Pb(II) adsorption on Fe_3O_4 magnetite nanoparticles, two simple kinetic models were tested.

The pseudo-first order rate expression, popularly known as the Lagergren equation, is generally described by the following equation (Lagergren, 1898):

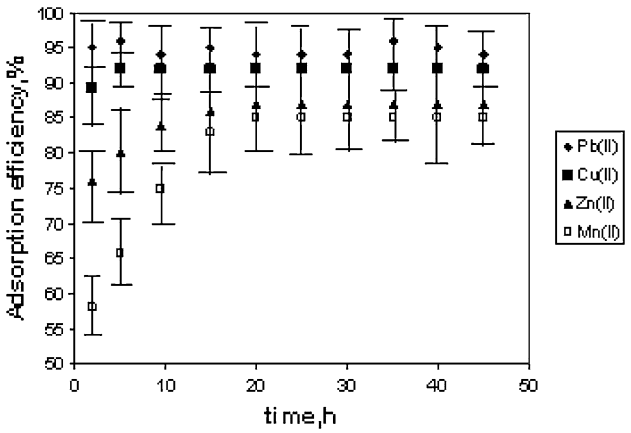

Fig. 5 Effect of contact time on the adsorption of Pb(II), Mn(II), Cu(II) and Zn(II) ions using magnetic Fe_3O_4 nanoparticles. T = 298 K, pH 5.5, adsorbent dosage = 200 mg, $V_{solution}$ = 50 mL, Initial metal ions concentration = 150 mg L^{-1}

$$\frac{dq}{dt} = k_{ad}(q_e - q) \tag{4}$$

where, q_e is the amount of the metal ions adsorbed at equilibrium per unit weight of sorbent (mg g^{-1}); q is the amount of metal ions adsorbed at any time (mg g^{-1}). Besides, k_{ad} is the rate constant (min^{-1}). Integrating with appropriate boundary conditions ($q = 0$ for $t = 0$ and $q = q_t$ for $t = t$), Eq. 4 takes the form:

$$\ln(q_e - q) = \ln q_e - k_{ad}t \tag{5}$$

However, if the intercept does not equal the natural logarithm of equilibrium uptake of metal ions, the reaction is not likely to follow a first-order path even if experimental data have high coefficient of determination (Lagergren, 1898). The coefficients of determination for all metal ions adsorption kinetic tests were found to be between 0.9434 and 0.9765 and were reported in Table 1 together with the Lagergren rate constants calculated from the slope of Eq. 5 (Ho and McKay, 1998).

The adsorption data was also analyzed in terms of a pseudo-second order mechanism given by (Hou et al. 2003; Marmier et al. 2000).

$$\frac{dq}{dt} = k_2(q_e - q)^2 \tag{6}$$

where, k_2 is the rate constant (mg g^{-1} min^{-1}). Integrating the above equation and applying boundary conditions (i.e. q = 0 for t = 0and q = q_t for t = t), gives:

$$\frac{t}{q_t} = \frac{1}{h_o} + \frac{1}{q_e}t \tag{7}$$

here, h_o is the initial adsorption rate. If the second-order kinetics is applicable, the plot of t/q against t in Eq. 7 should give a linear relationship from which the constants

Table 1 Lagergren rate equation constants and pseudo second-order rate equation constants for Mn(II), Zn(II), Cu(II) and Pb(II) adsorption on Fe_3O_4 magnetite nanoparticles

Metal ions	Pseudo first-order rate equation constants k_{ad} (× min)	q_e (exp.) (g mg^{-1})	SSE	R^2
Mn(II)	0.024	11.5	0.541	0.9654
Zn(II)	0.026	12.4	0.523	0.9434
Cu(II)	0.031	14.5	0.556	0.9687
Pb(II)	0.033	16.4	0.583	0.9765
Metal ions	Pseudo second-order rate equation constants h_o (× min g mg^{-1})	q_e(exp) (g mg^{-1})	SSE	R^2
Mn(II)	1234.5	22.5	0.017	0.9996
Zn(II)	1298.5	24.6	0.014	0.9994
Cu(II)	1345.6	25.6	0.008	0.9999
Pb(II)	1445.6	27.8	0.007	0.9999

q_e and h_o can be determined. Linear model gave a good fit to the experimental data. This means that the adsorption can be described by a pseudo-second order rate equation, hence q_e and h_o were evaluated and presented in Table 1. R^2 values are approximately the same for all the 4 metal ions, with values of about 0.999. In the limit at initial adsorption time, h_o is defined as (Ho and McKay 1998; Horsfall and Spiff 2004):

$$h_o = k_2 q_e^2 \tag{8}$$

h_o was calculated for the 4 metal ions and the values are reported in Table 1. The results obtained are similar to previous studies (Lagergren 1898; Ho and McKay 1998; Horsfall and Spiff 2004).

For all the regressions, the residual sum of squares (SSE), as the difference between the predicted values and the experimental data, can be calculated by the following equation:

$$\sum_n (q_e \exp - q_e calc)^2 \tag{9}$$

where the subscripts exp and calc refer to the experimental and the calculated q values, respectively. A lower SSE value indicates a lower discrepancy between the experimental and the estimated parameters, allowing to determine the best fitting model. Hence, the higher correlation coefficients (R^2) and lower SSE values for pseudo-second-order kinetic model indicated that the sorption followed a pseudo-second order mechanism, likely controlled by chemisorption (Araneda et al. 2008).

3.4 Effect of pH

The pH of the aqueous solution is an important controlling parameter in heavy metal ion adsorption processes, as reported by several authors in the literature. Fig. 6 shows the effect of solution pH in the range 2–7 on the removal of Pb(II), Cu(II), Zn(II) and Mn(II) ions from aqueous solutions by magnetite nanoparticles. As a matter of fact, at higher pH the determination of reliable adsorption capacity is not possible, due to the possible precipitation of cations as hydroxides.

Experiments were carried out at 298 K with a contacting time of 24 h. The adsorption efficiency increases by increasing the pH, for all the investigated cations. As an example, Pb(II) adsorption efficiency gradually increases from 75.7 % to 92.3 % when the pH increases from 2 to 7.

The results demonstrate that the cations removal was mainly dependent on the proton concentration in the solution. This has been previously attributed to the formation of surface complexes between the functional groups (≡FeOH) of the sorbent and, for example, the Pb(II) ions,

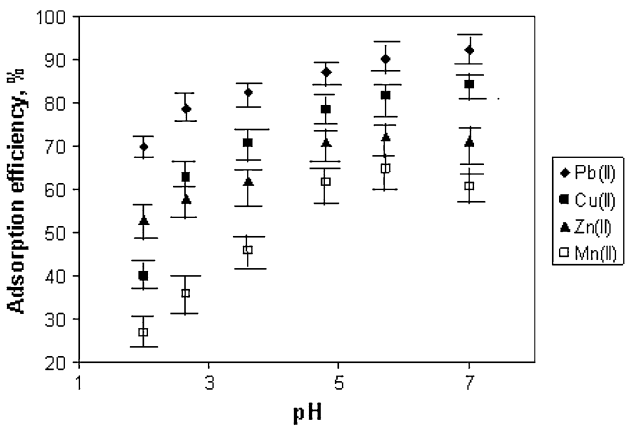

Fig. 6 The effect of pH on the adsorption of Pb(II), Cu(II), Zn(II) and Mn(II) ions onto magnetic Fe_3O_4 nanoparticles. T = 298 K, t = 24 h, adsorbent dosage = 200 mg, $V_{solution}$ = 50 mL, Initial metal ion concentration = 150 mg L^{-1}

with the possible reaction being expressed as follows (Hou et al. 2003):

$$sH_2O + q{\equiv}FeOH + rPb^{2+} \rightleftarrows ({\equiv}FeO)_qPb_r(OH)_s^{(2-q-s)} + (s+q)H^+ \quad (10)$$

where $({\equiv}FeO)_qPb_r(OH)_s^{(2-q-s)}$ corresponds to the surface complexes and s, q and r are the stoichiometric coefficients. When pH increases, this equilibrium shifts in such a manner that a greater number of sites are present in the more reactive deprotonated form, thereby leading to a higher uptake of Pb(II).

The results show very similar trends for Zn(II), Cu(II) and the Mn(II) adsorption efficiency; this pH dependency has been attributed to the formation of surface complexes similar to those reported in the equation (10) for Pb(II) cations.

Furthermore, from measured zeta potential of magnetite solution at different pH values, it appears that the magnetite surface has a positive charge at pH below 6.0 and a negative charge when pH is higher than 6.0 (Hou et al. 2003). This result is consistent with experimental data reported in Fig. 6.

Furthermore it should be noted that magnetite is an amphoteric solid, which can develop charges in the protonation (Fe–OH + H^+ ↔ Fe–OH_2^+) and deprotonation (Fe–OH ↔ Fe–O^- + H^+) reactions of Fe–OH sites on surface (Wang et al. 2011). The reactions can be written as:

$${\equiv}FeOH \rightleftarrows {\equiv}FeO^- + H^+ \quad K_{a1}^s \quad (11)$$

$${\equiv}FeOH_2^+ \rightleftarrows {\equiv}FeOH + H^+ \quad K_{a2}^s \quad (12)$$

and the corresponding acidity constants, as

$$K_{a1}^s = \frac{[H^+]\{{\equiv}FeO^-\}}{\{{\equiv}FeO\}} \quad (13)$$

$$K_{a2}^s = \frac{[H^+]\{{\equiv}FeOH\}}{\{{\equiv}FeOH_2^+\}} \quad (14)$$

where [ ] is the solution species concentration in mol L^{-1} and { } is the solid surface concentration in mol/g. According to the pH of the solution, the surface is charged differently and could behave as an anion or cation exchanger. It is important to realize that negative, positive, and neutral functional groups can coexist on magnetite surface. At pH < pH_{zpc}, the $FeOH_2^+$ groups predominate over the FeO^- groups, i.e., although the surface has a net positive charge, some FeO^- groups are still present. At the pH_{zpc}, the number of $FeOH_2^+$ groups equals the number of FeO^- groups and as the pH increases, the number of FeO^- groups increases (pH_{zpc} have been calculated but not reported here). It follows that magnetite particles may adsorb either negatively or positively charged species by electrostatic attraction depending on pH, even if, as previously reported, a complete analysis of all the pH interval is not possible dealing with cations.

Figure 6 shows that a magnitude of adsorption can be defined according to the following order: Mn < Zn < Cu < Pb. The uptake of Mn(II), Zn(II), Cu(II) and Pb(II) ions onto magnetite nanoparticles occurs by physico-chemical interactions, likely represented by electrostatic attractions. In particular, the size of hydrated ionic radii seems to influence the interactions with the negative charged adsorption site, as the greater the ion's hydration, the farther it is from the adsorbing surface and the weaker its adsorption (hydrated ionic radii: Pb^{2+}: 4.01 Å < Cu^{2+}: 4.19 Å < Zn^{2+}: 4.30 Å < Mn^{2+}: 4.43 Å) (Ko et al., 2004). Hence, Pb(II) has the lowest hydrated ionic radius and the highest capability to compete with proton and, hence, the highest comparative adsorption capacity.

The results obtained in this work in terms of metal adsorption capacity are of the same order of magnitude of those reported by other authors in the literature on the same sorbent (Wang et al. 2011; Yuan et al. 2009; Boddu et al. 2008; Yean et al. 2005). Although many different sorbents can be used for the same purpose, magnetic nanosorbents possess a number of unique physical and chemical properties and they are easily dispersed in aqueous solutions. A large number of their atoms are superficial atoms which are unsaturated and, hence, can determine high adsorption capacity towards several metal ions (Kalfa et al. 2009; Zhang et al. 2008; Liu et al. 2005). Magnetic particles can be removed very quickly from a matrix using a magnetic field, but they do not retain their magnetic properties when the field is removed (Wang et al. 2011). This system has also several advantages compared with conventional or other nano-adsorbents such as the absence of secondary wastes and the possible recycling of the materials involved on an industrial scale. Furthermore, the magnetic particles can be tailored to separate specific metal species in water, wastes or slurries (Yantasee et al. 2007; Ngomsik et al. 2006; Liu et al. 2008). However, from a practical point of view, there is a major drawback in the application of such nanomaterials for treating wastewater. Because the treatment of wastewater is usually conducted in a suspension of these nanoparticles, an additional separation step is required to remove them from a large volume of solution, resulting in increased operating costs.

3.5 Adsorption isotherms

Adsorption isotherms of Mn(II), Zn(II), Cu(II) and Pb(II) onto magnetite nanoparticles are reported in Fig. 7.

Under the above-mentioned conditions, the maximum adsorption capacity resulted to be 0.180 mmol g^{-1} for Pb(II), 0.170 mmol g^{-1} for Cu(II), 0.160 mmol g^{-1} for Zn(II), and 0.140 mmol g^{-1} for Mn(II), respectively. The

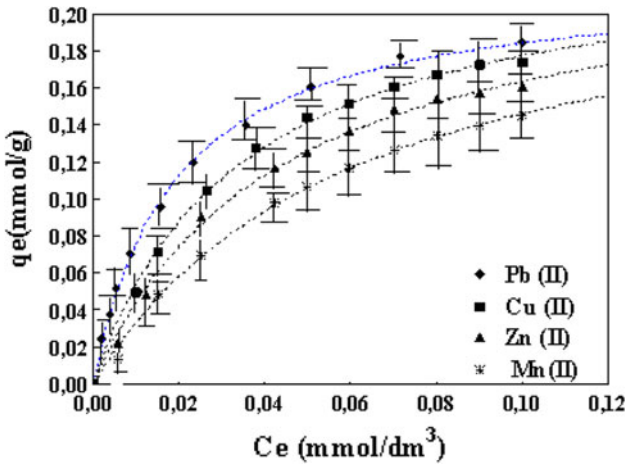

Fig. 7 Mn(II), Zn(II), Cu(II) and Pb(II) adsorption isotherms onto Fe_3O_4 magnetite nanoparticles. T = 25 °C, pH = 5.5 Comparison between experimental data and Langmuir model. $V_{solution}$ = 50 mL, Initial metal ion concentration = 150 mg L^{-1}

uptake of Mn(II), Zn(II), Cu(II) and Pb(II) ions onto magnetite nanoparticles occurs by physico-chemical interactions, likely represented by electrostatic attractions and the comparative adsorption magnitude is confirmed on the entire equilibrium concentration range.

A basic modelling analysis was carried out in order to determine the isotherm model that better describes the experimental data. In Table 2, Langmuir and Freundlich model parameters were reported, as derived from the regression analysis.

The Freundlich equation frequently gives an adequate description of adsorption data over a restricted range of concentration; it is usually suitable for a highly heterogeneous surface and an adsorption isotherm lacking of a plateau, indicating a multi-layer adsorption (Lagergren 1898). Values of 1/n less than unity indicate that a significant adsorption takes place at low concentration but the increase in the amount adsorbed with concentration becomes less significant at higher concentration and vice versa (Ho and McKay 1998).

The essential characteristic of the Langmuir isotherms can be expressed in terms of a dimensionless constant separation factor or equilibrium parameter, R_L, which is defined as (Farmer 1974):

$$R_L = \frac{1}{(1 + bC_o)} \quad (15)$$

where b is the Langmuir constant and C_o is the initial metal ion concentration. The value of R_L indicates the type of the isotherm to be either favorable ($0 < R_L < 1$), unfavorable ($R_L > 1$), linear ($R_L = 1$) or irreversible ($R_L = 0$). From our study, an initial metal ion concentration of 600 mg L^{-1}, R_L values for Pb(II), Cu(II), Mn(II) and Zn(II) ions adsorption ranged from 2.09 to 1.67, therefore, adsorption process is unfavorable.

As can be observed from data reported in Table 2, Langmuir model shows the highest comparative value of the coefficient of determination (R^2) and the lowest value for SSE, indicating a better approximation of model parameters to the experimental counterparts. In Fig. 7 the fitting of experimental data by Langmuir model was reported.

3.6 Effect of the temperature

For all the investigated ions, adsorption experiments were conducted varying the temperature between 15 °C and 40 °C under the following conditions: L/S = 1:4 and pH 5.5.

Figures 8a and b show the curves obtained for the adsorption tests at different time and temperature for Pb(II) and Zn (II) taken as example, respectively. As can be observed, for both ions, the adsorption capacity is greater for lower temperatures, as expected being adsorption an exothermic process. Moreover, the increase in adsorption capacity is higher for lowest values of temperature.

The temperature has an effect also on the time necessary to reach the equilibrium; a higher temperature, in fact, determines a lower equilibrium time.

Table 2 Estimated parameters for the Langmuir and Freundlich models for isotherm of Mn(II), Zn(II), Cu(II) and Pb(II) adsorption on Fe_3O_4 magnetite nanoparticles. T = 25 °C

Ions	Freundlich model $q = K_F c_{eq}^{\frac{1}{n}}$			Langmuir model $q = \frac{q_{max} b c_{eq}}{(1+b c_{eq})}$			
	K_F (mmol g^{-1})(L $mmol^{-1}$)$^{1/n}$	1/*n*	R^2	q_{max} (mg g^{-1})	b (L g^{-1})	R_L (L $mmol^{-1}$)	R^2
Mn(II)	0.144 ± 0.006	0.175 ± 0.002	0.9587	0.149 ± 0.007	1.37 ± 0.04	1.67	0.9987
Zn(II)	0.160 ± 0.009	0.178 ± 0.004	0.9643	0.177 ± 0.008	1.47 ± 0.05	1.77	0.9988
Cu(II)	0.173 ± 0.011	0.123 ± 0.003	0.9745	0.184 ± 0.005	1.68 ± 0.03	1.99	0.9988
Pb(II)	0.185 ± 0.013	0.112 ± 0.006	0.9876	0.189 ± 0.003	1.89 ± 0.04	2.09	0.9999

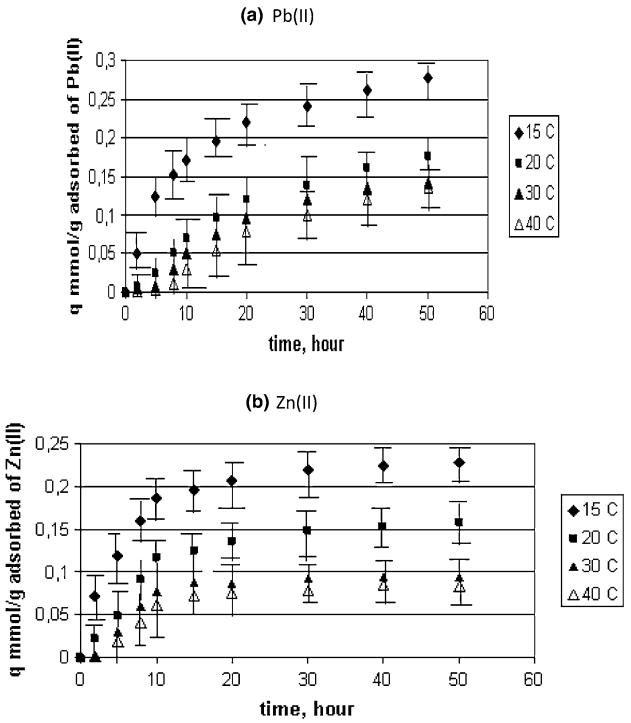

Fig. 8 The effect of temperature on the adsorption of Pb(II) (**a**) and Zn(II) (**b**) ions on the magnetic Fe_3O_4 nanoparticles; pH = 5.5, adsorbent dosage = 200 mg, Initial metal ions concentration = 150 mg L^{-1}

4 Conclusion

In this work, Fe_3O_4 nanoparticles were synthesized by co-precipitation method and used for treating a water artificially contaminated by metal ions, such as Pb(II), Cu(II), Zn(II) and Mn(II). Experimental results suggest that the adsorption capacity of Fe_3O_4 nanoparticles towards metal ions depends on the metal ions electronegativity. The maximum adsorption capacity in the investigated conditions was 0.180 mmol g^{-1} for Pb(II), 0.170 mmol g^{-1} for Cu(II), 0.160 mmol g^{-1} for Zn(II), and 0.140 mmol g^{-1} for Mn(II) respectively. Moreover, adsorption capacity seems to be strongly dependent on solution pH and temperature. The adsorption mechanism seems to be mainly an electrostatic attraction between metal ions and nanoparticles influenced by the hydrated ionic radius of the metal cations. The Langmuir model better interprets the adsorption data. A kinetic analysis showed that the adsorption of all the investigated ions onto Fe_3O_4 nanoparticles occurs by a pseudo-second order mechanism. In conclusion, it is here demonstrated that the Fe_3O_4 nanoparticles with fine grain size (<10 nm) can be efficiently used as an effective, convenient and low-cost material for the removal and recovery of metals from wastewater.

References

Ahn, Y., Choi, E.J., Kim, E.H.: Superparamagnetic relaxation in cobalt ferrite nanoparticles synthesized from hydroxide carbonate precursors. Rev. Adv. Mater. Sci. **5**, 477–480 (2003)

American Public Health Association: Standard Methods, Examination of water 3010. American Chemical Society, Washington DC (1995)

Araneda, C., Fonseca, C., Sapag, J., Basualto, C., Yazdani-Pedram, M., Kondo, K., Kamio, E., Valenzuela, F.: Removal of metal ions from aqueous solutions by sorption onto microcapsules prepared by copolymerization of ethylene glicol dimethacrylate with styrene. Sep. Purif. Technol. **6**, 517–523 (2008)

Banfield, J.F., Zhang, H.: Nanoparticles in the environment. In: Ribbe, P.H., Rossi, J.J. (eds.) Nanoparticles and the environment. The Mineralogical Society of America, Washington, DC (2001)

Balsamo, M., Di Natale, F., Erto, A., Lancia, A., Montagnaro, F., Santoro, L.: Cadmium adsorption by coal combustion ashes-based sorbents - relationship between sorbent properties and adsorption capacity. J. Hazard. Mater. **187**, 371–378 (2011)

Boddu, V., Abburi, K., Talbott, J., Smith, E., Haasch, R.: Removal of arsenic(III) and arsenic(V) from aqueous medium using chitosan-coated biosorbent. Water Res. **42**(3), 633–642 (2008)

Di Natale, F., Erto, A., Lancia, A., Musmarra, D.: A descriptive model for metallic ions adsorption from aqueous solutions onto activated carbons. J. Hazard. Mater. **169**(1–3), 360–369 (2009)

Farmer, V.C.: Recent advances in analytical infrared spectroscopy. Phil. Trans. R. Soc. Lond. A **305**, 609–619 (1982)

Farmer, V.C. (ed.): The Infrared Spectra of Minerals. Mineralogical Society, London (1974)

Faur-Brasquet, C., Kadirvelu, K., Le Cloirec, P.: Removal of metal ions from aqueous solution by adsorption onto activated carbon cloths: adsorption competition with organic matter. Carbon **40**, 2387–2392 (2002)

González, F., Bonilla, F.A., Zambrano, G., Gómez, M.E., Lopez, J.A.: Synthesis and characterization of Fe_3O_4 magnetic nanofluid. RLMM. **30**, 60–66 (2010)

Goya, G.F., Berquo, T.S., Fonseca, F.C., Morales, M.P.: Static and dynamic magnetic properties of spherical magnetite nanoparticles. J. Appl. Phys. **94**, 3520–3528 (2003)

Häfeli, U.O., Schütt, W., Teller, J., et al. (eds.): Scientific and Clinical Applications of magnetic Cariers. Plenum, New York (1997)

Ho, Y.S., McKay, G.: Sorption of dye from aqueous solution by peat. Chem. Eng. J. **70**, 115–124 (1998)

Horsfall, M., Spiff, A.I.: Studies on the effect of pH on the sorption of Pb^{2+} and Cd^{2+} ions from aqueous solutions by *caladium bicolor* (wild cocoyam) biomass. Electron. J. Biotech. **7**, 1–7 (2004)

Hou, Y.L., Yu, H.F., Gao, S.: Solvothermal reduction synthesis and characterization of superparamagnetic magnetite nanoparticles. J. Mater. Chem. **13**, 1983–1987 (2003)

Hua, L., Han, H., Chen, H.: Enhanced electrochemiluminescence of CdTe quantum dots with carbon nanotube film and its sensing of methimazole. Electrochim. Acta **54**(5), 1389–1394 (2009)

Jiang, J.Q.: Removing arsenic from groundwater for the developing world—a review. Water Sci. Technol. **44**, 89–98 (2001)

Kalfa, O.M., Yalçinkaya, Z., Turker, A.R.: Synthesis of nano B2O3/TiO2 composite material as a new solid phase extractor and its application to preconcentration and separation of cadmium. J. Hazard. Mater. **166**, 455–461 (2009)

Kang, C., Maeng, I.H., Oh, S.J., Son, J.H., Jeon, T.I., An, K.H., Lim, S.C., Lee, Y.H.: Frequency-dependent optical constants and conductivities of hydrogen-functionalized single-walled carbon nanotubes. Appl. Phys. Lett. **87**, 1–3 (2005)

Keith, K.H., McKay, G.: Study of arsenic(V) adsorption on bone char from aqueous solution. J. Hazard. Mater. **160**, 845–854 (2008)

Khajeh, M., Khajeh, A.: Synthesis of magnetic nanoparticles for biological and water applications. Int. J. Green Nanotechnol. Phys. Chem. **1**(1), 51–56 (2009)

Ko, D.C.K., Cheung, C.W., Keith, K.H., Choy, Porter, J.F., McKay, G.: Sorption equilibria of metal ions on bone char. Chemosphere **54**, 273–281 (2004)

Lagergren, S.: About the theory of so-called adsorption of soluble substances. K. Svenska Vetensk-Akad. Handl. **24**, 1–39 (1898)

Liu, S.X., Chen, X., Chen, X.Y., Liu, Z.F., Wang, H.L.: Activated carbon with excellent chromium (VI) adsorption performance prepared by acid–base surface modification. J. Hazard. Mater. **141**, 315–319 (2007)

Liu, Y., Liang, P., Guo, L.: Nanometer titanium dioxide immobolized on silica gel as sorbent for preconcentration of metals ions prior to their determination by inductively coupled plasma atomic emission spectrometry. Talanta **68**, 25–30 (2005)

Liu, H.L.Z., Peng, Z., Deng, L.: A novel technology for biosoprtion and recovery hexavalent chromium in wastewater by bio-functional magnetic beads. Bioresour. Technol. **99**, 6271–6279 (2008)

Marmier, N., Delisée, A., Fromage, F.: Sorption of Cs(I) on magnetite in the presence of silicates. J. Colloid Interface Sci. **223**, 83–88 (2000)

Mohan, D., Singh, K.P.: Single - and multi-component adsorption of cadmium and zinc using activated carbon derived from bagasse-an agricultural waste. Water Res. **36**, 2304–2318 (2002)

Moreno-Piraján, J.C., Giraldo, L.: Heavy metal ions adsorption from wastewater using activated carbon from orange peel. J. Chem. **9**(2), 926–937 (2012)

Moreno, J.C., Gómez, R., Giraldo, L.: Removal of Mn, Fe, Ni and Cu ions from wastewater using cow bone charcoal. Materials **3**, 452–466 (2010)

Nasiruddin Khan, M., Farooq Wahab, M.: Characterization of chemically modified corncobs and its application in the removal of metal ions from aqueous solution. J. Hazard. Mater. **141**, 237–244 (2007)

Nassar, N.N., Hassan, A., Pereira-Almao, P.: Application of nano-technology for heavy oil upgrading: catalytic steam gasification/cracking of asphaltenes. Energy Fuels **25**, 1566–1570 (2011a)

Nassar, N.N., Hassan, A., Pereira-Almao, P.: Metal oxide nanoparticles for asphaltene adsorption and oxidation. Energy Fuels **25**, 1017–1023 (2011b)

Nassar, N.: Kinetics, equilibrium and thermodynamic studies on the adsorptive removal of nickel, cadmium and cobalt from wastewater by supermagnetic iron oxide nano-adsorbents. Can. J. Chem. Eng. **9999**, 1–8 (2011)

Ngomsik, A.F., Bee, A., Siaugue, J.M., Cabuil, V., Cote, G.: Nickel adsorption by magnetic alginate microcapsules containing an extractant. Water Res. **40**, 1848–1856 (2006)

Niemeyer, C.M.: Nanoparticles, proteins, and nucleic acids: biotechnology meets materials Science. Angew. Chem. Int. Ed. **40**, 4128–4158 (2001)

Palacin, S., Hidber, P.C., Bourgoin, J.-P., Miramond, C., Fermon, C., Whitesides, G.M.: Patterning with magnetic materials at the micron scale. Chem. Mater. **8**, 1316–1321 (1996)

Pankhurst, Q.A., Connolly, J., Jones, S.K., Dobson, J.: Applications of magnetic nanoparticles in biomedicine. J. Phys. D **36**, R167–R181 (2003)

Pattanayak, J., Mondal, K., Mathew, S., Lalvani, S.B.: A parametric evaluation of the removal of As(V) and As(III) by carbon-based adsorbents. Carbon **38**, 589–596 (2000)

Perez, J.M.: Iron oxide nanoparticles: hidden talent. Nat. Nanotechnol. **2**, 535–536 (2007)

Portet, D., Denizot, B., Rump, E.: Nonpolymeric coatings of iron oxide colloids for biological use as magnetic resonance imaging contrast agents. J. Colloid Interface Sci. **238**, 37–42 (2001)

Purevsuren, B., Avid, B., Narangerel, J., Gerelmaa, T., Davaajav, Ya.: Investigation on the pyrolysis products from animal bone. J. Mater. Sci. **9**, 737–740 (2004)

Puziy, A.M., Poddubnaya, O.I., Zaitsev, V.N., Konoplitska, O.P.: Modeling of heavy metal ion binding by phosphoric acid activated carbon. Appl. Surf. Sci. **221**, 421–429 (2004)

Reimer, P., Weissleder, R.: Development and experimental use of receptor specific MR contrast media. Radiology **36**, 153–163 (1996)

Roco, M.C.: Nanotechnology: Convergence with modern biology and medicine. Curr. Opin. Biotechnol. **14**, 337–346 (2003)

Savage, N., Diallo, M.S.: Nanomaterials and water purification: opportunities and challenges. J. Nanopart. Res. **7**, 331–342 (2005)

Shen, Y.F., Tang, J., Nie, Z.H., Wang, Y.D., Ren, Y., Zuo, L.: Preparation and application of magnetic Fe_3O_4 nanoparticles for wastewater purification. Sep. Purif. Technol. **68**, 312–319 (2009)

Si, S., Kotal, A., Mandal, T.K., Giri, S., Nakamura, H., Kohara, T.: Size-controlled synthesis of magnetite nanoparticles in the presence of polyelectrolytes. Chem. Mater. **16**, 3489–3496 (2004)

Sun, S.H., Murray, C.B., Weller, D., Folks, L., Moser, A.: Monodisperse FePt nanoparticles and ferromagnetic FePt nanocrystal superlattice. Science **287**, 1989–1992 (2000)

Sun, S.H., Zeng, H.: Size-controlled synthesis of magnetite nanoparticles. J. Am. Chem. Soc. **124**, 8204–8205 (2002)

Tratnyek, P.G., Johnson, R.L.: Nanotechnologies for environmental clean up. Nano Today **1**, 44–48 (2006)

Wan, S.R., Huang, J.S., Yan, H.S., Liu, K.L.: Size-controlled preparation of magnetite nanoparticles in the presence of graft copolymers. J. Mater. Chem. **16**, 298–303 (2006)

Wang, X.S., Lu, H.J., Liu, F., Ren, J.J.: Adsorption of lead(II) ions onto magnetite nanoparticles. Adsorpt. Sci. Technol. **26**, 407–417 (2011)

Waychunas, G.A., Kim, C.S., Banfield, J.F.: Nanoparticulate iron oxide minerals in soils and sediments: unique properties and contaminant scavenging mechanisms. J. Nanopart. Res. **7**, 409–433 (2005)

Wilson, J.A., Pulford, I.D., Thomas, S.: Sorption of Cu and Zn by bone charcoal. Environ. Geochem. Health **25**, 51–56 (2003)

Wu, F.C., Tseng, R.L., Juang, R.S.: Comparisons of porous and adsorption properties of carbons activated by steam and KOH. J. Colloid Interface Sci. **283**, 49–56 (2005)

Xie, J., Xu, C., Kohler, N., Hou, Y., Sun, S.H.: Controlled pegylation of monodisperse Fe_3O_4 nanoparticles for reduced non-specific uptake by macrophage cells. Adv. Mater. **19**, 3163–3166 (2007)

Yantasee, W., Warner, C.L., Sangvanich, T.: Removal of heavy metals from aqueous system with thiol functionalized superparamagnetic nanoparticles. Environ. Sci. Technol. **41**, 5114–5119 (2007)

Yean, S., Cong, L., Yvuz, C.T., Mayo, J.T., Yu, W.W.: Effect of magnetite particle size on adsorption and desorption of arsenite and arsenate. J. Mater. Res. **20**, 3255–3264 (2005)

Yuan, C., Hung, C.-H., Chen, K.-C.: Electrokinetic remediation of arsenate spiked soil assisted by CNT-Co barrier—The effect of barrier position and processing fluid. J. Haz. Mat. **171**, 563–570 (2009)

Zhang, Q., Pan, B., Zhang, W., Jia, K., Zhang, Q.: Selective sorption of lead, cadmium and zinc ions by a polymeric cation exchanger containing nano-Zr(HPO3S)2. Environ. Sci. Technol. **42**, 4140–4145 (2008)